Research Article

Facile preparation of wearable heater based on conductive silver paste with low actuation voltage and rapid response

Siqi Zhao[1] · Bowen Li[1,2] · Tengfei Li[1,2] · Chenghao Deng[1]

Received: 16 July 2020 / Accepted: 9 November 2020 / Published online: 19 November 2020

Abstract
Towards emerging electric heaters for wearable electronics, actuators and high-performance heating systems, various properties including flexibility, low actuation voltage, rapid response, facile adaptability, thermal and mechanical stability are highly desired. Herein, a high-performance heater based on commercial conductive silver paste is proposed, through quite simple scrape coating, painting and pen writing. Benefiting from its excellent viscosity, the silver paste can be firmly coated on a variety of substrates, even including hydrophobic and oleophobic polytetrafluoroethylene and cotton thread of high curvature. After curing the silver paste, the silver nanoflakes inside are encapsulated in a polymer framework and are closely interconnected, forming a reliable conductive network with low sheet resistance (minimum 0.18Ω/sq). This structure protects the silver nanoflakes from oxidation and provides this flexible silver heater (FSH) excellent thermal and mechanical stabilities, as demonstrated by long-time heating, cyclic heating and multiple deformation tests. The FSH achieves high surface temperature (280 °C) at a low operation voltage (2 V), with rapid thermal response time (less than 7 s). The application demonstrations of FSHs in custom-shaped wearable heaters and heating patterns, thermal therapy, flexible heating thread and thermal switch suggest the distinct advantages of FSHs in flexible and wearable devices.

Keywords Electric heater · Silver paste · High-performance · Rapid response · Facile adaptability

1 Introduction

Electric heaters based on Joule thermal effect of electric conductors have been used in local heating for over a century. Nowadays, the development of flexible conductive materials injects new vitality to the Joule effect based heaters. Personal and industrial applications of electric heaters include wearable devices [1–3], personal thermal management [4–6], soft actuators [7, 8], drug release [9], defrosting [10–13], thermochromic display device [14] and industry heating system [15].

The future development of emerging flexible heaters puts requirements on flexibility, transparency, rapid response, low actuation voltage, high heating temperature, facile adaptability, mechanical and thermal reliabilities [16–19], which always rely on the low electrical resistance, high thermal conductance, size scale, robust mechanical properties and thermal stability of materials.

Conventional metals with high electrical and thermal conductivities are efficient for traditional heaters. However, the mechanical stiffness and poor adaptability limit their application in emerging flexible heaters. Indium tin oxide (ITO) film has been used as a transparent conductor for decades of years. However, ITO film is not available for wearable or rapid response heater due to its brittleness and low thermal conductivity. In this case, a variety of nanomaterials and their structures have been employed to solve the issues mentioned above, including carbon

✉ Chenghao Deng, cdeng@gxu.edu.cn | [1]Center On Nanoenergy Research, School of Physical Science and Technology, Guangxi University, Nanning 530004, P. R. China. [2]CAS Center for Excellence in Nanoscience, Beijing Key Laboratory of Micro-Nano Energy and Sensor, Beijing Institute of Nanoenergy and Nanosystems, Chinese Academy of Sciences, Beijing 100083, China.

nanotubes (CNTs) [20, 21], graphene [22, 23], 2D transition-metal carbide [10], metal meshes [24, 25], conductive polymers [26, 27], metal nanowires [28–31] and their mixtures [18, 32–35]. Owing to high electrical conductivity and excellent mechanical properties, CNTs and graphene have been first explored in the application of flexible heaters. Zhang et al. reported a graphene-based heater [22], which reached steady-state temperature 247.3 °C in 20 s at 18 V actuation voltage. After folding the heater for 100 times, the output temperature remained precisely controlled. They demonstrated its application in flexible and custom-shaped heaters. Kim et al. prepared a CNT-based heater using solution processing. The heater produced over 100 °C temperature at 7 V supplied voltage [20]. A heater based on the hybrid of graphene and CNTs was also reported [36], achieving 85 °C maximum temperature at 12 V actuation voltage. 10,000 bending cyclic tests suggested the excellent mechanical and thermal stabilities of this heater. However, carbon nanomaterials-based heaters all suffer from high actuation voltage due to relative high electrical resistance. For about 100 °C surface temperature, carbon nanomaterials-based heaters always need 4 ~ 20 V actuation voltage and 20 ~ 40 s heating time to achieve this temperature [17, 22, 37, 38]. Towards safe and biological applications, flexible heaters with lower actuation voltage (< 5 V) are desired, which promote the rise of nanometallic materials-based heaters.

Silver nanowires are promising elements for flexible heaters due to much lower electrical resistance of networked silver nanowires compared to CNTs and graphene. By embedding silver nanowires into thin polyvinyl alcohol (PVA) film and cold-pressing them to adjust their sheet resistance, Lan et al. fabricated a flexible heater with sheet resistance of 26Ω/sq [28]. The temperature of this heater reached 74 °C in 20 s at a bias of 5 V and showed excellent stability after being kept at the environment with 80 °C temperature and 80% humidity for half a year. Jang et al. spin-coated silver nanowires on a PET substrate and obtained a heater with 1.3Ω/sq sheet resistance. The temperature of this heater reached 250 °C at 4.5 V supplied voltage [39]. In addition to silver nanowires, copper nanowires were also developed to fabricate much cheaper and more stable flexible heaters. A transparent copper nanowire-based heater reported by Tian et al. attained 50 °C at 5 V actuation voltage [30].

In general, high temperatures (maximum 200 ~ 260 °C) induced at low voltage (2.5 ~ 4.0 V) for silver nanowires-based heaters are acquired [16, 39, 40]. Even so, silver nanowires-based heaters are faced with three problems: (1) Surface oxidation of silver nanowires at high temperature. (2) Low melting point of silver nanowires. (3) Weak interface adhesion between silver nanowires and substrate, making them picky about the substrate.

To solve these problems, efforts to pack silver nanowires insider more thermally stable materials, or to mix silver nanowires and substrate together as a whole, have been done. Zhou et al. fabricated a flexible heater based on Ag@Pt alloy-walled hollow nanowires to achieve high thermal stability at 400 °C for 11 h and mechanical stability with 5000 cycles bending, but the fabrication process was complex with a cost of noble metal [41]. Tian et al. developed a tri-layer rGO/Ag nanowire/GO composite film, preventing silver nanowires from oxidation [35]. The tri-layer film-based heater can reach 148 °C with highly thermal stability during cycling heating and long-time working (> 5 h). Ma et al. proposed a heater by mixing silver nanowires and aramid nanofibers together through vacuum filtration and hot-pressing [16]. The heater showed sufficient heating reliability and stability during long-time and repeated heating. These methods are effective but make the fabrication process complicated.

Conductive silver paste is a commonly used material in electronic industry, which is usually used to repair the electrical circuit and is user-friendly. The commercial silver paste contains silver nanoflakes, resin, curing agent and addiction agents. The excellent viscosity of resin makes the silver paste can be coated on a majority of substrates, including super hydrophobic or oleophobic materials such as polytetrafluoroethylene (PTFE), which will be discussed later. Moreover, the silver paste can be painted on any object, no matter what the shape and texture are. This character benefits the free customization of heaters. After curing at low temperature, a framework encapsulating the silver nanoflakes inside will be formed due to the polymerization of resin monomer. This framework closely packs the silver nanoflakes and protects them from oxidation during heating process. In this research, we use commercial conductive silver paste as ink to directly paint, or draw, or write conductive films and flexible silver heaters (FSHs) by one step on a variety of flexible substrates, demonstrating the shape and substrate adaptability of the heaters. The substrates include polyimide (PI), polyethylene terephthalate (PET), PTFE, polyvinyl chloride (PVC), paper, glass and cotton thread. These heaters achieve high surface temperature (280 °C) at low actuation voltage (2 V), with rapid thermal response time (less than 7 s), excellent mechanical and thermal stabilities (> 800 cyclic bending and 4 h heating). The preparation process needs no special treatments. Except for the curing process (about 20 min), we can prepare a FSH in 1 min. The potential applications for FSHs in wearable devices, personal thermal management are demonstrated. A thermal switch based on the heater using PTFE film as substrate is designed.

2 Experimental section

2.1 Preparation of FSHs

The silver paste used in this research was purchased from SINWE Corporation, which contains effective silver paste and thinner. Their mass ratio is 1: 0.7. The density of the silver paste is 2.0 g/cm^3. The contents of silver nanoflakes, epoxy resin, amine curing agent, butyl acetate and other additional agents in effective silver paste are 75%, 12%, 2%, 8% and 3%, respectively. The silver paste was first filled into injectors and pens, which were prepared for painting or drawing FSHs. Then, we dropped a small amount (0.01 ~ 0.025 mL) of silver paste onto a 2 cm × 2 cm flexible substrate, including PI, PET, PVC, PTFE, glass and paper substrates. After that, we used a plastic blade to scrape the silver paste to form a film, which was then cured at 80 °C for 20 min. Then, a FSH was obtained. Except for scrape coating, we can also directly write or draw a conductive film using silver paste pen. The preparation process is schematically illustrated in Fig. 1.

2.2 Electrothermal characterization of FSHs.

We used a DC power source (HITECH -IT6922A) to supply DC voltage (current) to FSHs and measured their electrical resistance simultaneously. Commercial copper tapes were attached to FSHs as connection electrodes. After applying 0.1 ~ 2.5 V heating bias to FSHs, an IR thermal meter (Fluke 62 max$^+$) and an IR thermal Imager (HIK Vision, H10) were used to measure the temperature and its distribution on FSHs.

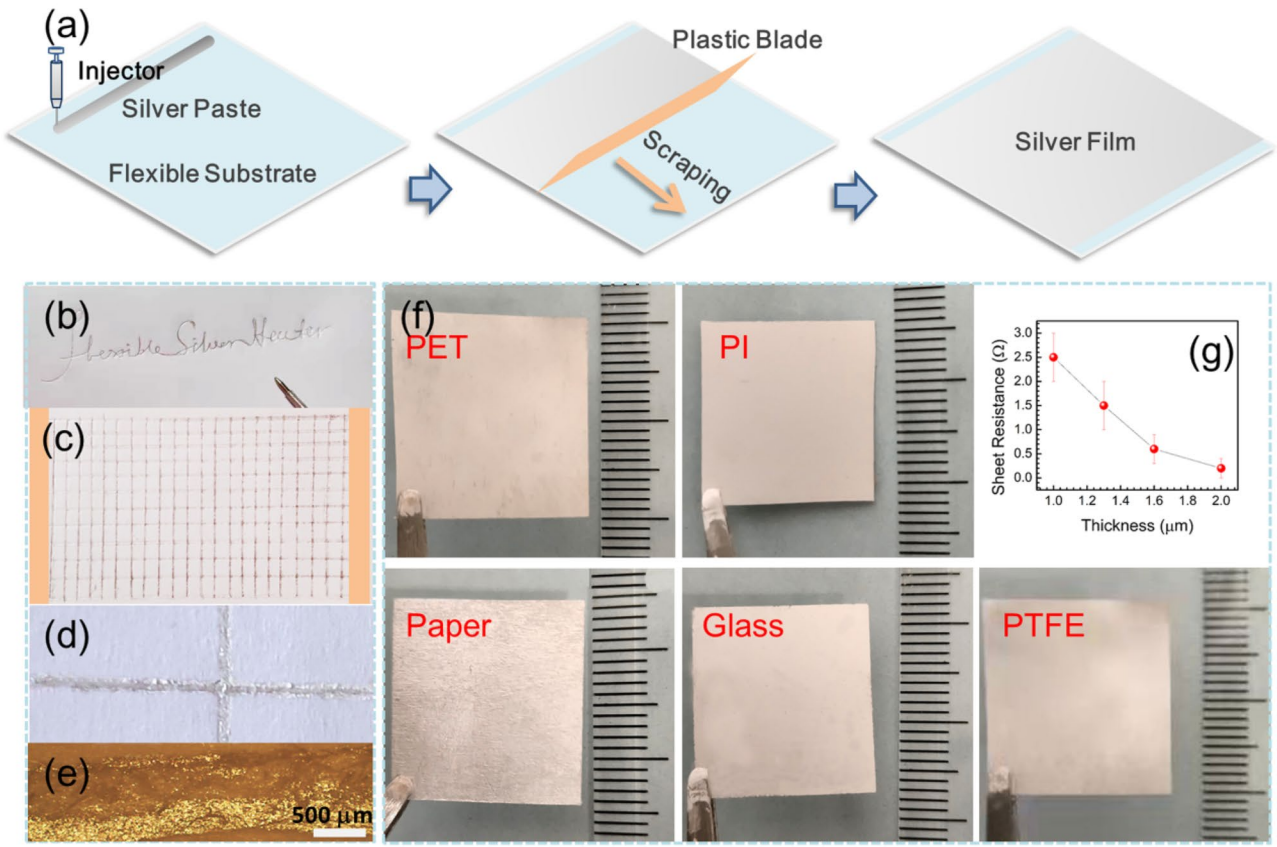

Fig. 1 **a** Preparation schematic of FSH using scrape coating. **b** The words "Flexible Silver Heater" written on a common paper using a homemade silver paste pen. **c** Conductive silver grid drawn by the silver paste pen. **d** Partially enlarged photograph and **e** microscope image of this conductive grid. **f** Photographs of FSHs prepared using five typical flexible substrates, including PET, PI, paper, glass and PTFE substrates. **g** Relationship between the sheet resistance of FSHs prepared on PI substrates and the thickness of silver film

3 Results and discussion

3.1 Morphology, microstructure and resistance of scrape-coated FSHs

Figure 1a shows the schematic illustration of preparing FSH by scrape coating. At first, 0.01 ~ 0.025 mL silver paste was squeezed out onto a 2 cm × 2 cm square flexible substrate gradually to form a line, with the help of an injector. Then, a plastic blade was employed to scrape the silver paste line gently. When a uniform film was formed, the blade was removed. After scrape coating, a curing process was carried out to form a solidified FSH. Two different curing methods were employed, which are room temperature (RT) curing for 24 h and 80 °C curing for 20 min. Figure 1f presents the FSHs prepared on five typical flexible substrates using 0.025 mL silver paste, which are PET, PI, paper, glass and PTFE substrates. Although the five substrates have quite different surface energy, uniform and reliable silver films are formed on all substrates, benefiting from the excellent viscosity of epoxy resin in silver paste. The epoxy resin enhances the adhesion strength between silver film and substrate, making the silver film shape and substrate adaptable. In addition to the five substrates-based FSHs mentioned above, PVC and cotton thread-based FSHs were also prepared, which will be discussed later.

The volume of silver paste droplet determines the thickness of the silver film after curing process. Figure 1g reveals the relationship between the sheet resistance of PI-based FSHs and the thickness of silver films. With the thickness increasing from 1 to 2μm, the sheet resistance decreases rapidly from 2.5 to 0.2Ω/sq. The formation of silver film is a balance between the internal force of silver paste and the interfacial adhesion. When the volume of silver paste droplets is less than 0.01 mL(0.0025 mL/cm^2), the formed silver film is not continuous, leading to nonconductive film. When the volume is larger than 0.025 mL (0.00625 mL/cm^2), the silver paste will be too redundant for scrape coating. To obtain smaller sheet resistance, we can employ layer by layer coating. According to this result, we can estimate that the required volume of silver paste for fabricating a 0.01 m^2 heater (the size of a commercial hot pack) with 0.5Ω/sq sheet resistance is about 0.5 mL.

Other than scrape coating on various substrates, we can also use the silver paste as conductive ink to write conductive paths. The viscosity of the silver paste used in this research is about 20,000 CPS. The drawn patterns will be conductive when the pen ballpoint is larger than 8 mm. Figure 1b presents the words "Flexible Silver Heater" written by a homemade pen using the silver paste as ink. Figure 1c shows a conductive grid drawn by this homemade pen. Figure 1d and e shows the partially enlarged photograph and a microscope image of this conductive grid. The line width is about 7.5 ± 0.8 mm, with line resistance of 182 ± 43 Ω/cm measured at different positions. The line width and resistance of these drawn patterns are not uniform. To reduce the line resistance and improve the uniformity, we can adopt repeated writing, or use a pen with larger ink pump capacity.

We used an X-ray photoelectron spectroscopy (XPS, Thermo Fisher Scientific, ESCALAB 250XI +) and a scanning electron microscope (SEM, Hitachi SU8220) to characterize the morphologies and chemical structures of silver films. Figure 2d shows two SEM images of the silver films formed on PI substrates. The silver film is made up of stacked silver nanoflakes and the polymer binding them together. The lateral size of the nanoflakes is about 0.5 ~ 3μm. The film thickness is about 2μm, as measured from Fig. 2f. Figure 2a shows the wide scan XPS spectra of the silver films cured at RT and 80 °C. For the silver film cured at RT, five silver peaks can be observed, which consist of one Ag 4p peak, two Ag 3d peaks and two Ag 3p peaks. C 1 s, O 1 s and N 1 s peaks can also be observed. However, after heating at 80 °C for 20 min, the Ag peaks and N peak almost disappear and two silicon peaks arise. We attribute this difference to the polymerization of epoxy resin and silicone coupling agent in the silver paste at 80 °C.

The first step of the curing process is the volatilization of thinner. Then, the epoxy bonds will be broken and transform into hydroxide radicals with the help of amine curing agent. This process can be accomplished at RT, resulting in low molecular weight polymerization. At this state, the polymer still has fluid nature to some extent. Thus, for the silver films cured at RT, a mass of silver nanoflakes could be exposed during XPS measurement, resulting in high silver peaks in XPS. The peak of C 1 s for RT cured silver films consists of three types of carbon bonds, which are C–C bond, C–O bond and C = O bond. C–O bond comes from the epoxy group and hydroxide radical. C = O bond comes from the non-volatilized thinner.

At relatively higher temperature, further polymerization is proceeded. The molecules with hydroxide radicals combined with each other, through the broken of hydroxide radicals and the formation of reticular C–O–C bonds. This polymerization process produces a polymer framework and closely packs the silver nanoflakes in this framework [42]. The silver flakes are encapsulated in the polymer framework, which results in the disappearance of the Ag peaks while XPS only represents the surface chemical information within 5 nm depths. While the epoxy groups and hydroxide radicals on the surface transform into inner reticular C–O–C bonds, the content of C–O bonds in C 1 s peak decreases. The content of C = O bond also decreases

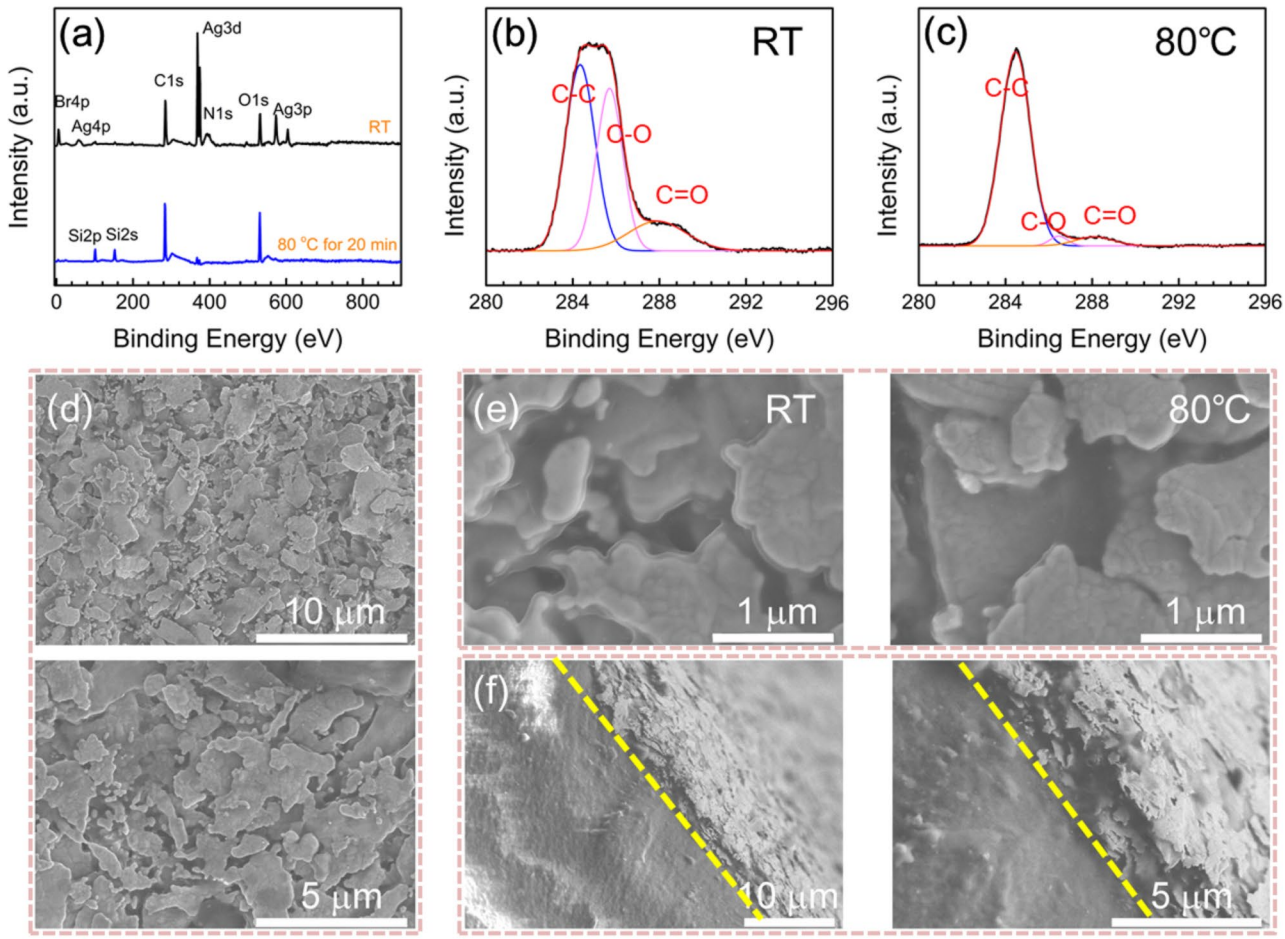

Fig. 2 **a** XPS wide scan spectra of silver films. High-resolution XPS spectra of C1s for the silver films cured at **b** RT and **c** 80 °C. **d** SEM images of the silver films on PI substrate. **e** High-resolution SEM images to address the difference of the silver films cured at RT and 80 °C. **f** SEM images of the cross-section of the silver film on PI substrate

with the volatilization of thinner. From the SEM image of the RT cured silver film in Fig. 2e, an organic membrane between the silver nanoflakes can be observed, which may consist of non-volatilized thinner and unpolymerized molecules with epoxy groups or hydroxide radicals. For the 80 °C cured silver film, this type of membrane between silver nanoflakes almost disappears.

With the formation of the polymer framework during curing process, the thickness of silver film decreases and the interconnection between silver flakes becomes closer and closer. As consequences, more conductive paths and lower sheet resistance are acquired. For the RT cured silver films prepared using 0.025 mL silver paste droplet, the sheet resistance ranges from 1 ~ 2 Ω/sq. After 80 °C curing for 20 min, the sheet resistance decreases to about 0.2 Ω/sq. The framework of epoxy resin encapsulates and fixes the silver nanoflakes, protecting the silver flakes from oxidation and maintaining the stability of conductive paths. These characteristics make the silver film thermally and mechanically stable, which help to extend the service life of FSHs.

3.2 Electrothermal characterization of FSHs

After scrape coating silver films on flexible substrates, we used a DC power source to investigate the Joule heating behavior of FSHs, as shown in Fig. 3a. Copper tapes were used as connection electrodes. 0.1 ~ 2.5 V bias was applied to FSHs. An infrared thermometer was used to measure the surface temperature of FSHs. According to energy conservation law, the heat generated by Joule heating is equal to the dissipated heat, which involves three main processes: heat absorption, heat convection and heat radiation. The governing equation can be described as [3],

$$\frac{\partial(\rho c_p T)}{\partial t} = \frac{U^2}{RAd} - \frac{h}{d}(T - T_0) - \frac{\varepsilon\sigma(T^4 - T_0^4)}{d} \quad (1)$$

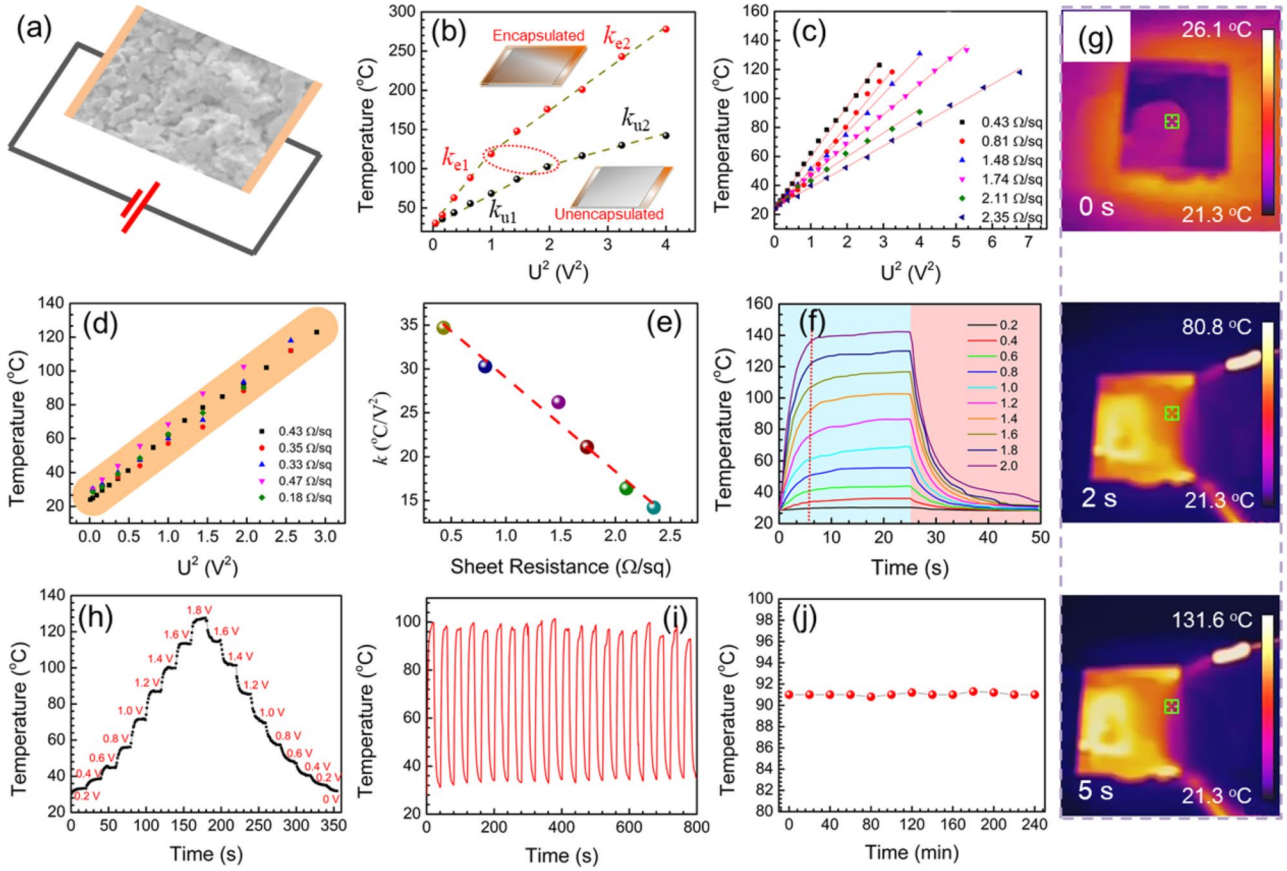

Fig. 3 **a** Schematic illustration of electrothermal characterization for FSHs. **b** The relationship between current-induced temperature rise (T) and supplied voltage (U^2) of a PI-based FSH sample (sample 1) before and after encapsulation**. c** T–U^2 curves of six FSH samples with different sheet resistance. **d** T–U^2 curves of five FSH samples with sheet resistance smaller than 0.5 Ω/sq. **e** Relationship between the slope (k) of T–U^2 curves for the six FSH samples in (**c**) and their sheet resistance. **f** Temperature evolution with time of sample 1 at different supplied voltages. **g** IR thermal images of sample 1 after supplying 2 V bias for 0, 2 and 5 s. **h** Step, **i** cyclic and **j** long-time heating tests of sample 1

where ρ, c_p, A, d, ε and R are the mass density, specific heat, area, thickness, effective heat emissivity and electrical resistance of FSH, respectively. U is the supplied heating bias. T and T_0 are the surface temperature of FSH and the environmental temperature, respectively. h is the convective heat-transfer coefficient. σ is the Stefan-Boltzmann constant. In the air, heat convection between FSH and air dominated the heat dissipation. The temperature of FSHs in this research is lower than 600 K. By this temperature, the influence of heat radiation is estimated to be less than 0.5%. Thus, the item of heat radiation can be neglected. The heat conduction equation is simplified into,

$$\frac{\partial(\rho c_p T)}{\partial t} = \frac{U^2}{RAd} - \frac{h}{d}(T - T_0) \tag{2}$$

Then, the time-dependent temperature can be derived as,

$$T = T_0 + \frac{U^2}{RhA}(1 - e^{-(h/\rho d c_p)t}) \tag{3}$$

With time increasing, the temperature of FSH becomes saturated. The temperature rise at saturation stage is expressed as,

$$\Delta T = T - T_0 = \frac{U^2}{RhA} \tag{4}$$

That is, the temperature rise (ΔT) is proportional to U^2 and h^{-1}, when the resistance and area of FSH are two constants.

Figure 3b shows the relation between Joule heating induced temperature (T) and U^2 of a PI-based heater (sample 1). The sheet resistance of this FSH sample is 0.4 Ω/sq. There are two temperature rising curves, corresponding to the sample before and after encapsulation. Compared to the unencapsulated heater, the encapsulated heater is covered by a flexible substrate on the surface, forming

a substrate-silver film-substrate sandwich structure. This flexible substrate is acted as a heat shield, which helps to reduce the heat convection between the heater and air, increasing the temperature at 2 V from 140 to 280 °C dramatically.

Each curve has two linear regions, with a turning point around 110 K. This turning point may be attributed to the change of the electrical contact between connection electrodes and the silver film, which may be ascribed to the thermal expansion of substrate under high temperature. The slope of the linear curve is $1/hRA$. The slopes of these four regions are named k_{e1}, k_{e2}, $k_{u1}$and k_{u2}, which are marked in Fig. 3b. The values of these four slopes are 93, 51, 37 and 20 °C/V^2, respectively. As the resistance and the area of the FSH sample are invariable, it is calculated that the convective heat-transfer coefficient (h) is reduced by 60% after encapsulation.

Figure 3c shows the linear T–U^2 curves of six unencapsulated FSHs with different sheet resistance ($0.43 \sim 2.35\Omega$/sq). At a fixed bias, the induced temperature increases with sheet resistance reducing. However, for the FSHs with sheet resistance smaller than 0.5Ω/sq, there is no obvious difference in T–U^2 curves for different FSH samples, as shown in Fig. 3d. That could come from the limit of coating technique and the measurement error of our resistance meter, which needs further research. The T–U^2 curves can be fitted into a uniform formula, expressed as $T = 35.5U^2 + 23.5$ (°C). Figure 3e shows the slope (k) of the six T–U^2 curves in Fig. 3c. With sheet resistance increasing from 0.43 to 2.35 Ω/sq, k decreases linearly. The linear relation is expressed as $k = 39.65R - 10.67$ (°C/V^2). As k is equal to $1/hRA$, the convective heat-transfer coefficient h can be expressed as $h^{-1} = 0.016R^2 - 0.004R$. Thus, h is not a constant, but varies with the sheet resistance of FSHs.

Figure 3f shows the temperature evolution with time for sample 1 at different supplied voltages (0.2 ~ 2 V). At $t = 0$ s, a bias was fed onto the FSH sample, then the temperature increases exponentially as Eq. (4) describes. The time for the FSH achieving almost stable temperature is less than 7 s, which is quite fast among the similar heaters as we know. At different supplied voltages, the temperature evolutions take almost the same time to reach stability. At $t = 25$ s, the supplied voltage is cutoff, then the temperature of the FSH decreases down rapidly. Figure 3g shows us the infrared (IR) thermal images of sample 1 during heating. The square in the images is sample 1. At $t = 0$ s without heating, the temperature of the sample is a little lower than environmental temperature. After supplying 2 V bias, the maximum temperature on the sample reaches 80 °C in 2 s and reaches 130 °C in 5 s. Uniform temperature distribution on the sample's surface can be observed. Figure 3h shows the step tests of sample 1. Step voltage from 0.2 to 1.8 V with 0.2 V step is fed to the sample. Every step lasts for 20 s. Stable and clear temperature steps can be observed. At a same supplied voltage, the temperature of the descending stage is only 1 ~ 2 °C higher than that of the ascending stage. This result demonstrates the rapid response and the excellent controllability of the FSH.

Figure 3i is the cyclic test results of sample 1 under 1.4 V bias. The period of the supplied voltage is 40 s. During the 20 cyclic heating tests, the maximum temperature of each cycle ranges from 93 to 100 °C, while the minimum temperature of each cycle keeps stable around 34 °C. Figure 3j demonstrates the thermal stability of the sample under long-time heating. During 4 h heating tests, the temperature of the sample keeps around 91 °C very steadily.

In Table 1, we compare the heating performance of FSH with the heaters achieved in previous studies with different materials. When the temperature rise is related to actuation voltage and heater area, we use heat efficiency ($\Delta T \times A/U^2$) to describe the heating ability. As presented in the table, the silver paste-based heater in our work show outstanding heating performance, benefiting from the excellent electrical and thermal conductivity.

Flexibility is an important indicator for FSH. We measured the performance of FSH under different degrees of bending and repeated bending. Figure 4c shows a PET-based FSH sample (sample 2) fixed on a sliding rail. The sheet resistance and the area of the sample are 1.8 Ω and 2.0 cm × 5.1 cm, respectively. The supplied voltage is 2 V. The FSH can be bent to different degrees. Figure 4d presents the IR thermal images of sample 2 bending to different degrees, while a slight temperature rise of the FSH under bending is observed. Figure 4a shows the change of maximum surface temperature of sample 2 and its electrical resistance change under different degrees of bending. The $\Delta L/L_0 \left(L/L_0 = 1 - L/L_0\right)$ in Fig. 4a means the relative distance change during bending tests between the two fixed ends shown in Fig. 4c. The resistance of the FSH remains exactly unchanged under bending, but the

Table 1 Properties of flexible heater using different materials

Nanomaterials	Heat efficiency(°C cm^2/V^2)	Response time(s)(~)	Reference
Graphene	50.2	30	[15]
PEDOT Coated Cotton	0.56	20	[6]
PEDOT	4.34	200	[26]
GuZr Metallic Glass	12.65	70	[12]
Copper Fiber	3.07	70	[13]
Metal Meshes	2.62	15	[24]
MXene (Ti_3C_2Tx)	2.64	45	[10]
Ag Nanowire/Aramid Fiber	224	15	[16]
Silver Paste	255	7	This Work

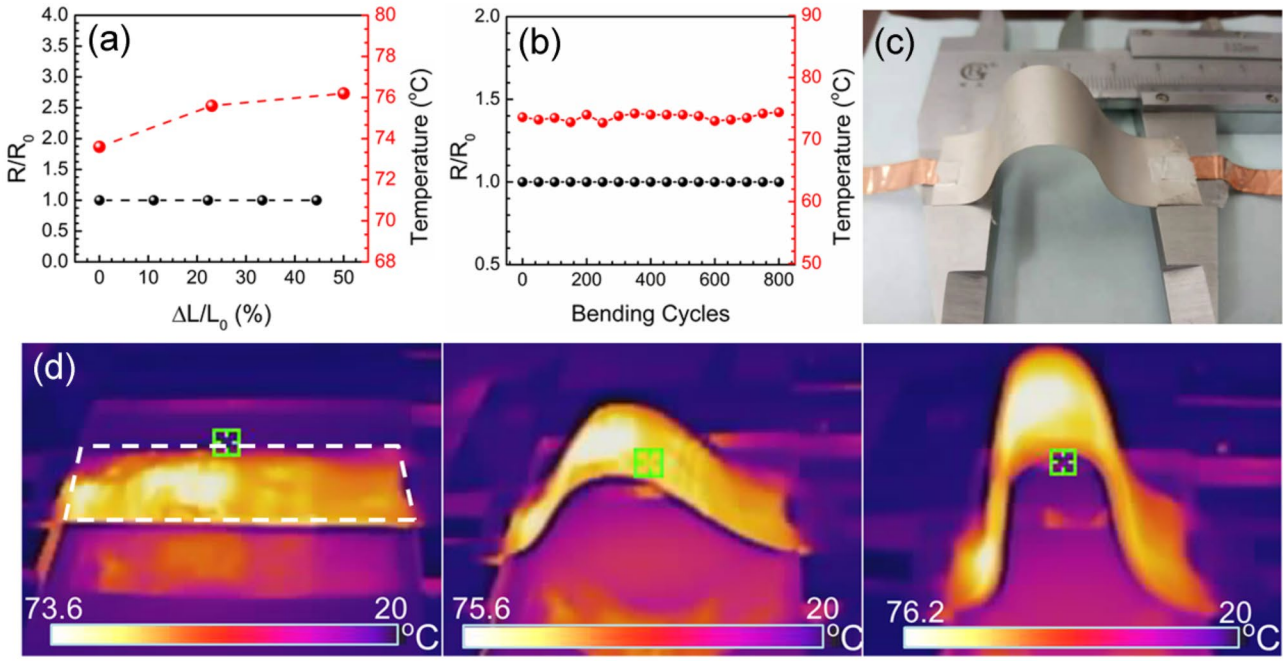

Fig. 4 **a** Electrical resistance and temperature change of a FSH sample (sample 2) under different bending degrees. **b** Electrical resistance and temperature change of sample 2 under cyclic bending. **c** Photograph of sample 2 and apparatus for bending test. **d** IR thermal images of sample 2 under different bending degrees, where the supplied bias is 2 V

maximum temperature of the FSH increases from 73.6 to 76.2 °C when the distance between the fixed ends decreases by 50%. We attribute this slight temperature rise to the closeness of the left and the right half parts, which helps to reduce the heat convection.

Figure 4b shows the stable resistance and temperature of sample 2 under cyclic bending. During the 800 cyclic bending tests, the initial resistance (the resistance of the FSH when the sample is straight without bending) of the sample remains exactly unchanged. The temperature shows 1.2 °C float around 73.6 °C and no tendency to increase or decrease is observed. This float may come from our measurement error. In addition, the flexibility of the heater has not shown any observable change during the long-time cyclic tests. Cyclic bending tests demonstrate the excellent flexibility, thermal and mechanical stabilities of FSHs.

3.3 Applications of FSHs: demonstration of the facile adaptability

Towards practical applications, flexibility, shape adaptability and low operation voltage are required. Figure 5 shows some typical applications of FSHs. Above discussions have demonstrated that the FSH can be operated at the voltage below 2 V. Here, we use 1.5 V as operation voltage, which is equal to the voltage of a commercial battery. Benefiting from the excellent viscosity of epoxy resin, the silver paste can be painted on most of the common substrates and painted into custom-shaped patterns as well. The left image in Fig. 5a presents a pattern of the abbreviation of our university on a common paper (GuangXi University) written by the silver paste, where we draw a dashed line to make the pattern clear. Using copper tapes as connection electrodes, we applied a 1.5 V bias to the pattern. The right image in Fig. 5a is the IR thermal image of the "GXU" pattern, where a maximum 99.3 °C is obtained. The nonuniform thermal pattern is a result of nonuniform resistance distribution. Nevertheless, this result demonstrates the superior adaptability of using silver paste to fabricate flexible heater.

Figure 5b presents the application of FSHs in thermotherapy. We use a medical adhesive patch as substrate to fabricate FSH. After painting the silver paste on it, the flexibility of the patch is barely affected. It can be attached to the body perfectly. We applied a 1.0 V operation voltage to this patch using copper tapes as connection electrodes. Fairly uniform temperature distribution is acquired and the maximum temperature of this FSH is 49.3 °C at this operation voltage. We do not use 1.5 V as operation voltage here is because the induced temperature at 1.5 V of this heater is too hot for human skin (around 85 °C).

For the FSHs in Figs. 5c and d, we adopted PVC as substrate, due to its ultra-soft texture which makes it skin

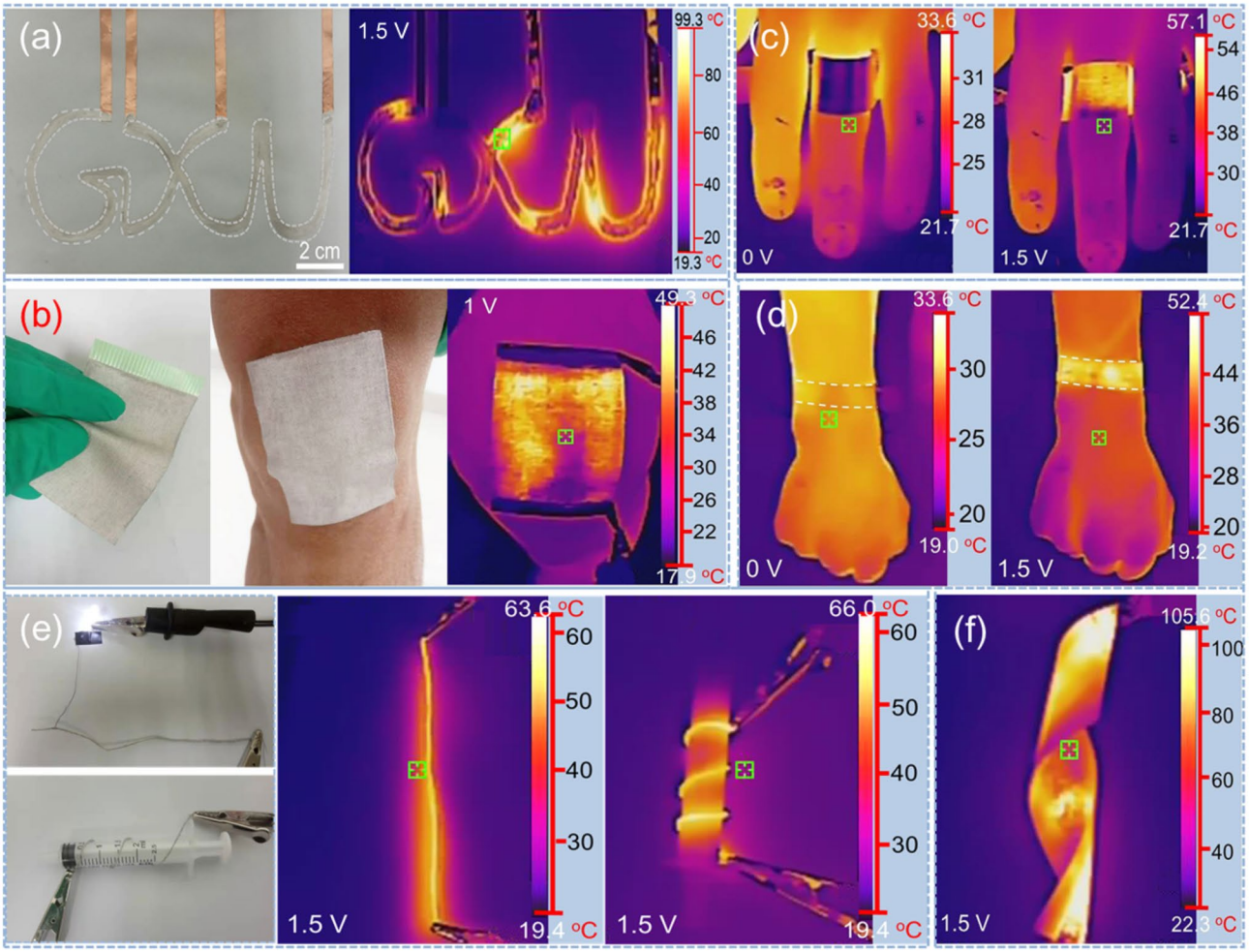

Fig. 5 **a** Photograph and IR thermal image of a "GXU" pattern painted using silver paste. **b** Photographs and IR thermal image of a medical adhesive patch based heater for thermal therapy. IR thermal images of **c** a ring-shaped heater and **d** a wristband-shaped heater before and after supplying 1.5 V voltage. **e** A conductive thread prepared by coating silver paste on cotton thread and its IR thermal images when it is straight or rolled up. **f** IR thermal image of a twisted heater at 1.5 V bias

conformable. Figure 5c shows a ring-shaped heater. Under 1.5 V operation voltage, its surface temperature is around 57 °C. Figure 5d shows a wristband-shaped heater. The temperature of this heater reaches 52 °C at 1.5 V operation voltage. The two temperature values are suitable for wearable devices to relieve pain and stiffness, which always need 41–77 °C heating temperature. Except for bending, the FSH can be also twisted, as shown by the FSH sample in Fig. 5f. The heater's temperature keeps around 100 °C at 1.5 V during twist and shows no temperature degradation after repeated twist. The resistance of the heaters mentioned above is ranged from 1 to 3 Ω. If we take 50 °C as suitable temperature for human, then an ordinary commercial No. 5 battery with 2500 mAh capacity can support these heaters by 1.6 ~ 5.0 h.

Except for the coating on a planar substrate, we can also coat the silver paste on high curvature surface, such as cotton thread, which can be easily accomplished by immersing the cotton thread into silver paste. After coating and curing processes, a flexible conductive thread with line resistivity of 0.57 Ω/cm is obtained. The original diameter of the thread is about 0.8 mm and increases by about 0.04 mm after coating. The left image in Fig. 5e shows the photograph of a light-emitting diode (LED) driven by a DC voltage using this silver thread as conductive wire. When we applied a 1.5 V bias to this 8.5 cm long thread, a 63.6 °C maximum surface temperature is obtained, as shown in the middle image of Fig. 5e. Compared to similar heaters as reported, the actuation voltage of this silver conductive thread for producing approximate temperature is reduced by one order [10]. The silver conductive thread maintains the excellent flexibility of cotton thread. As shown in Fig. 5f, we roll the

thread heater up and its surface temperature slightly increases to about 66 °C at the same 1.5 V bias.

3.4 Thermal switch based on FSH

As mentioned above, the substrates used for fabricating FSHs in this research include hydrophobic and oleophobic PTFE film. In addition to the hydrophobicity and oleophobicity, high thermal expansion coefficient is another characteristic of PTFE film. Using a heating platform, we measured that the length expansion of the PTFE film used in this research reaches 2% at 100 °C. Thus, we can use Joule heating to control the thermal expansion of PTFE-based FSHs. From this basic point, we designed a thermal switch using this PTFE-based FSHs. As shown in Fig. 6a, we coat silver paste on the both sides of a PTFE film. The silver film on one side is used as heating layer, while that on the other side is used as connecting electrode of the switch. The side used as heating layer is attached firmly onto a rigid substrate with a hole in the center. Thus, the part of film aligned to the hole is not fixed. When we apply a bias to the silver heating layer, the part aligned to the hole will bulge due to thermal expansion. We fabricated two identical structures and fixed them together face to face, with a small gap (about several tens of micrometers) between them. Before applying any bias to the heating layer, the connecting layers of the two parts are separated. The switch is on "OFF" state. When we apply a bias to the two parts simultaneously, the parts of the PTFE films aligned to the holes will bulge and make the two connecting layers contact to each other. Then, the switch is on "ON" state.

We used a LED to express the state of the switch. When we apply a voltage to heat the switch, the LED is lighted up, as shown in Fig. 6b. When the switch is on "On" state (applying a 1.5 V heating voltage), the temperature of the PTFE film is about 67 °C, as illustrated in Fig. 6d. Figure 6d presents the current evolution of the switch circuit during the process of applying and withdrawing heating voltage. At first, the current is zero, indicating the "OFF" state of the switch. At $t = 12$ s, a 1.5 V bias is supplied to the heating layer. After 5 s delay, the switch circuit is on. The bias applied to the switch circuit is also 1.5 V. Upon heating, the resistance (current) of switch circuit decreases (increases) rapidly due to the closer contact of the two connecting electrodes. At $t = 40$ s, the heating voltage is withdrawn. After 4 s delay, the resistance of the switch circuit begins to increase and becomes infinite after 27 s delay when the connecting layers are separated again. The switch shows stable performance during several heating and cooling cycles. After repeated thermal expansion and contraction, the resistance and the induced temperature of the heating

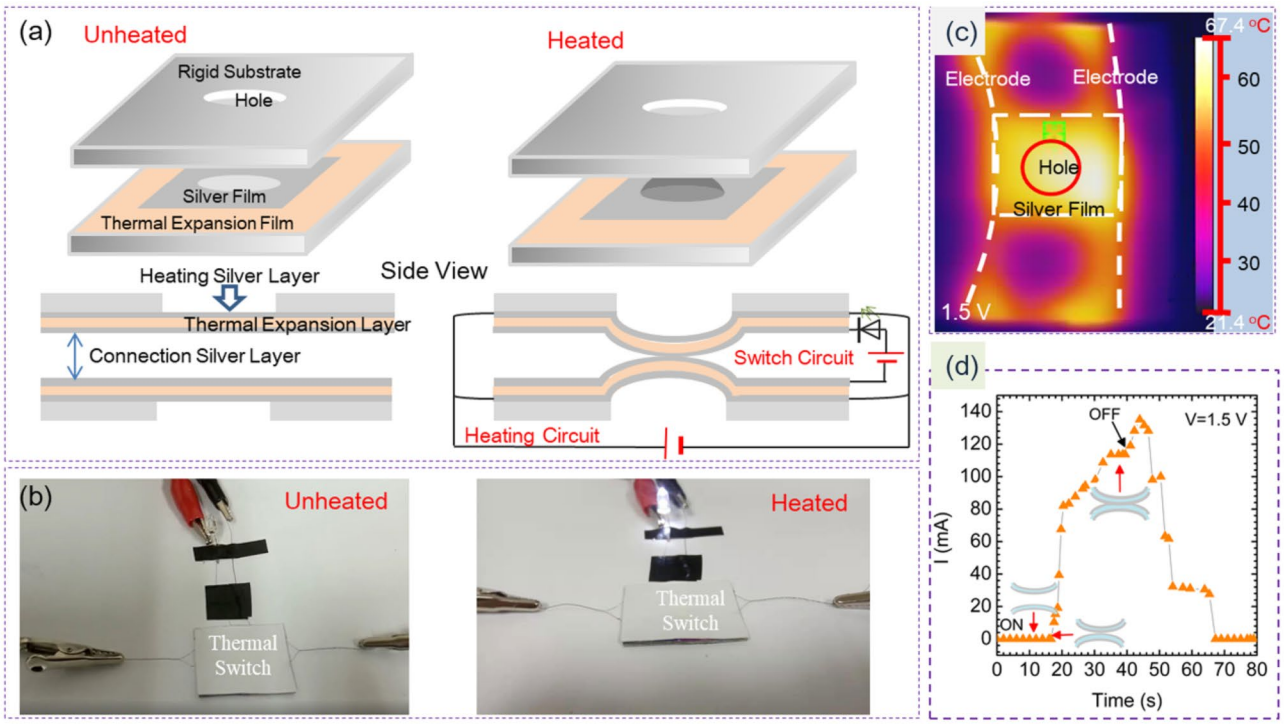

Fig. 6 **a** Schematic illustration of the thermal switch. **b** Photograph of the thermal switch before and after applying heating voltage. The LED is lighted up after applying heating voltage. **c** IR thermal image of the thermal switch when applying a 1.5 V heating voltage. **d** Current evolution with time of the switch circuit during the process of applying and withdrawing the heating voltage

layers remain unchanged. The FSH can be a feasible and reliable element for new type switches and actuators.

4 Conclusions

In this paper, a substrate and shape adaptable, thermally and mechanically stable, rapid response flexible heater with high performance based on commercial conductive silver paste is proposed and investigated. Due to the excellent viscosity of epoxy resin, the silver paste shows facile adaptability. It can be coated, painted, or written into desired shapes on a variety of substrates by a simple step. The used substrates include PI, PET, PVC, common paper, glass, oleophobic and hydrophobic PTFE and high curvature cotton thread. The polymer framework formed by curing the epoxy resin provides protection for the silver nanoflakes sealed inside and invests excellent thermal and mechanical stabilities to the FSHs, which are demonstrated by cyclic heating, long-time heating, cyclic bend and twist tests. The surface temperature of a FSH with sheet resistance of 0.4 Ω/sq reaches 280 °C at a low actuation voltage of 2 V, which is prominent in reported heaters. FSHs show rapid thermal response, with response time less than 7 s. The rapid response and the slight temperature difference (within 2 °C) between the ascending and descending heating stages demonstrate the excellent controllability of FSHs. The application demonstrations of FSHs in ring or wristband-shaped wearable heaters, thermal therapy, custom-shaped heating patterns, flexible heating thread and thermal switch suggest the distinct advantages of FSHs in flexible and wearable devices.

Acknowledgements This work was supported by the National Natural Science Foundation of China (No.11904058) and Scientific Research and Technology Development Program of Guangxi (No. AD19245118).

Compliance with ethical standards

Conflict of interest The authors declare no conflict of interest.

References

1. Lin S, Zhang T, Lu Q, Wang D, Yang Y, Wu X, Ren T (2017) High-Performance Graphene-Based Flexible Heater for Wearable Applications. Rsc Adv 7:27001–27006
2. Jang N, Kim K, Ha S, Jung S, Lee H, Kim J (2017) Simple Approach to High-Performance Stretchable Heaters Based on Kirigami Patterning of Conductive Paper for Wearable Thermotherapy Applications. Acs Appl Mater Interfaces 9:19612–19621
3. Cheng Y, Zhang H, Wang R, Wang X, Sun J (2016) Highly Stretchable and Conductive Copper Nanowire Based Fibers with Hierarchical Structure for Wearable Heaters. Acs Appl Mater Interfaces 8:32925–32933
4. Hsu P, Liu X, Liu C, Xie X, Lee H, Welch A, Zhao T, Cui Y (2015) Personal Thermal Management by Metallic Nanowire-Coated Textile. Nano Lett 15:365–371
5. Xie S, Li T, Xu Z, Wang Y, Liu X, Guo W (2018) A High-Response Transparent Heater Based on A CuS Nanosheet Film with Superior Mechanical Flexibility and Chemical Stability. Nanoscale 10:6531–6538
6. Zhang L, Baima M, Andrew T (2017) Transforming Commercial Textiles and Threads into Sewable and Weavable Electric Heaters. Acs Appl Mater Interfaces 9:32299–32307
7. Hyeonseok K, Habeom L, Inho H, Jinwook J, Phillip W, Hyunmin C, Junyeob Y, Sukjoon H, Seungyong H, Jinhyeong K (2018) Color-Changing Soft Actuators: Biomimetic Color Changing Anisotropic Soft Actuators with Integrated Metal Nanowire Percolation Network Transparent Heaters for Soft Robotics. Adv Funct Mater 28:1870220
8. Jiang S, Guo W, Liu S, Huang X, Li Y, Li Z, Wu H, Yin Z (2019) Grab and Heat: Highly Responsive and Shape Adaptive Soft Robotic Heaters for Effective Heating of Objects of Three-Dimensional Curvilinear Surfaces. Acs Appl Mater Interfaces 11:47476–47484
9. Pooria M, Ali T, Rahim R, Manuel O, Akbar K (2017) Smart Bandage for Monitoring and Treatment of Chronic Wounds. Small 14.
10. Park TH, Yu S, Koo M, Kim H, Kim EH, Park JE, Ok B, Kim B, Noh SH, Park C (2019) Shape-Adaptable 2D Titanium Carbide (MXene) Heater. ACS Nano 13:6835
11. Yoon S, Khang D (2016) Facile Patterning of Ag Nanowires Network by Micro-Contact Printing of Siloxane. Acs Appl Mater Interfaces 8:23236
12. An B, Gwak E, Kim K, Kim Y, Jang J, Kim J, Park J (2016) Stretchable, Transparent Electrodes as Wearable Heaters Using Nanotrough Networks of Metallic Glasses with Superior Mechanical Properties and Thermal Stability. Nano Lett 16:471–478
13. Jo H, An S, Lee J, Park H, Al-Deyab S, Yarin A, Yoon S (2017) Highly flexible, stretchable, patternable, transparent copper fiber heater on a complex 3D surface. NPG Asia Mater 9:e347–e347
14. Liu P, Zhou D, Wei Y, Jiang K, Wang J, Zhang L, Li Q, Fan S (2015) Load Characteristics of a Suspended Carbon Nanotube Film Heater and the Fabrication of a Fast-Response Thermochromic Display Prototype. ACS Nano 9:3753–3759
15. Tian S, He P, Chen L, Wang H, Ding G, Xie X (2017) Electrochemical Fabrication of High Quality Graphene in Mixed Electrolyte for Ultrafast Electrothermal Heater. Chem Mater 29:6214–6219
16. Ma Z, Kang S, Ma J, Shao L, Wei A, Liang C, Gu J, Yang B, Dong D, Wei L, Ji Z (2019) High-Performance and Rapid-Response Electrical Heaters Based on Ultraflexible, Heat-Resistant and Mechanically Strong Aramid Nanofiber/Ag Nanowire Nanocomposite Papers. ACS Nano 13:7578–7590
17. Di W, Li D, Min Z, Yang X, Wei Q (2018) Multifunctional Wearable Smart Device Based on Conductive Reduced Graphene Oxide/Polyester Fabric. Appl Surf Sci 454:218–226
18. Meng X, Chen T, Li Y, Liu S, Pan H, Ma Y, Chen Z, Zhang Y, Zhu S (2019) Assembly of carbon nanodots in graphene-based composite for flexible electro-thermal heater with ultrahigh efficiency. Nano Res 10:2498–2508
19. Zhang M, Wang C, Liang X, Zhe Y, Zhang Y (2017) Wearable Electronics: Weft-Knitted Fabric for a Highly Stretchable and Low Voltage Wearable Heater. Adv Electro Mater. https://doi.org/10.1002/aelm.201700193
20. Kim Y, Lee HR, Saito T, Nishi Y (2017) Ultra-Thin And High-Response Transparent And Flexible Heater Based on Carbon Nanotube Film. Appl Phys Lett 110:153301
21. Li Y, Zhang Z, Li X, Zhang J, Lou H, Shi X, Cheng X, Peng H (2017) A Smart, Stretchable Resistive Heater Textile. J Mater Chem C 5:41–46

22. Zhang T, Zhao H, Wang D, Wang Q, Pang Y, Deng N, Cao H, Yang Y, Ren T (2017) A Super Flexible And Custom-Shaped Graphene Heater. Nanoscale 9:14357–14363
23. Karim N, Zhang M, Afroj S, Koncherry V, Potluri P, Novoselov KS (2018) Graphene-Based Surface Heater for De-icing Applications. Rsc Adv 8:16815–16823
24. Lordan D, Burke M, Manning M, Martin A, Amann A, O'Connell D, Murphy R, Lyons C, Quinn A (2017) Asymmetric Pentagonal Metal Meshes for Flexible Transparent Electrodes and Heaters. Acs Appl Mater Interfaces 9:4932–4940
25. Liu Y, Su S, Chen L S, Yun Z, Huang W (2016) High-Performance Transparent Film Heater with An Embedded Ni Metal-mesh Based on Selected Metal Electrodeposition Process. SPIE/COS Photonics Asia: 10019.
26. Gueye M, Carella A, Demadrille R, Simonato J (2017) All-Polymeric Flexible Transparent Heaters. Acs Appl Mater Interfaces 9:27250–27256
27. Jeong O, Konishi S (2008) Three-Dimensionally Combined Carbonized Polymer Sensor And Heater. Sens Actu A Phys 143:97–105
28. Lan W, Chen Y, Yang Z, Han W, Zhou J, Zhang Y, Wang J, Tang G, Wei Y, Dou W (2017) Ultraflexible Transparent Film Heater Made of Ag Nanowire/PVA Composite for Rapid-Response Thermotherapy Pads. Acs Appl Mater Interfaces 9:6644–6651
29. Celle C, Mayousse C, Moreau E, Basti H, Carella A, Simonato J (2012) Highly Flexible Transparent Film Heaters Based on Random Networks of Silver Nanowires. Nano Res 5:427–433
30. Zhang H, Wang S, Tian Y, Wen J, Hang C, Zheng Z, Huang Y, Ding S, Wang C (2020) High-efficiency extraction synthesis for high-purity copper nanowires and their applications in flexible transparent electrodes. Nano Mater Sci 2:164–171
31. Zhang H, Wang S, Tian Y, Liu Y, Wang C (2020) Electrodeposition fabrication of Cu@Ni core shell nanowire network for highly stable transparent conductive films. Chem Engin J 390:124495
32. Kang J, Jang Y, Kim Y, Cho S, Suhr J, Hong B, Choi J, Byun D (2015) An Ag-Grid/Graphene Hybrid Structure for Large-Scale, Transparent, Flexible Heaters. Nanoscale 7:6567–6573
33. Kim D, Zhu L, Jeong D, Chun K, Bang Y, Kim S, Kim J, Oh S (2013) Transparent Flexible Heater Based on Hybrid of Carbon Nanotubes And Silver Nanowires. Carbon 63:530–536
34. Park J, Han D, Choi S, Kim Y, Kwak J (2019) Flexible Transparent Film Heaters Using A Ternary Composite of Silver Nanowire, Conducting Polymer and Conductive Oxide. RSC Adv 9:5731–5737
35. Tian Y, Wang C, Hang C, Huang Y, Chao L (2019) Chemical and thermal robust tri-layer rGO/Ag NWs/GO composite film for wearable heaters. Comp Sci & Techno 174:76–83
36. Li L, Hong SK, Jo Y, Tian M, Woo CY, Kim S, Kim J, Lee H (2019) Transparent, Flexible Heater Based on Hybrid 2D Platform of Graphene and Dry-Spun Carbon Nanotubes. ACS Appl Mater Interfaces 11:16223–16232
37. Lee Y, Le VT, Kim J, Kang H, Suh D (2018) Versatile, High-Power, Flexible, Stretchable Carbon Nanotube Sheet Heating Elements Tolerant to Mechanical Damage and Severe Deformation. Adv Funct Mater 28:1706007
38. Han J, Kim B, Woo J, Jang J, Cho J, Jeong H, Jeong S, Seo S, Lee G (2017) Bioinspired Multifunctional Superhydrophobic Surfaces with Carbon-Nanotube-Based Conducting Pastes by Facile and Scalable Printing. Acs Appl Mater Interfaces 9:7780–7786
39. Jang J, Hyun B, Ji S, Cho E, An B, Cheong W, Park J (2017) Rapid Production of Large-Area, Transparent And Stretchable Electrodes Using Metal Nanofibers As Wirelessly Operated Wearable Heaters. NPG Asia Mater 9:e432
40. Pyo K, Kim J (2016) Transparent And Mechanically Robust Flexible Heater Bbased on Compositing of Ag Nanowires And Conductive Polymer. Composit Sci Technol 133:7–14
41. Zhou K, Han C, Li C, Jiu J, Yang Y, Li L, Wang H, Liu J, Liu Z, Yan H (2018) Highly Stable Transparent Conductive Electrodes Based on Silver-Platinum Alloy-Walled Hollow Nanowires for Optoelectronic Devices. ACS Appl Mater & Interf 10:36128–36135
42. Liu W, Qiu Q, Wang J, Huo Z, Sun H (2008) Curing Kinetics And Properties of Epoxy Resin-Fluorenyl Diamine Systems. Polymer 49:4399–4405